

**Physically Adsorbed Monolayers\***

F. Y. WU (伍法岳)

*Department of Physics, Northeastern University, Boston  
Massachusetts 02115, U. S. A.*

AND

CHIA-WEI WOOT (吴家璋)

*Department of Physics, University of Illinois  
Urbana, Illinois 61801, U. S. A.*

(Received June 15, 1971)

We review in this article the basic theory of physical adsorption, and discuss relevant recent experimental and theoretical developments. As a concrete model we consider helium monolayers adsorbed on the surface of a crystalline argon crystal. Results on recent quantum mechanical calculations on heat of adsorption and band widths are presented. Effect of correlation is also estimated. A number of quantum statistical models are examined and their relative merits discussed in explaining the observed heat capacity data of helium monolayers.

---

**I. INTRODUCTION**

THE physical adsorption of noble gas atoms on crystalline substrates has been of historical interest to surface physicists. During the last several years, more reliable measurements on the properties of physically adsorbed monolayers have become available, stimulating renewal interest as well as controversy. As a result, a Symposium on Thin Helium Films was held in June, 1970, at Stevens Institute of Technology (Hoboken, New Jersey, U. S. A.), The Proceedings<sup>(1)</sup> of the Symposium had hardly appeared in print when new and peculiar phenomena were further observed.<sup>(2)</sup>

It is beyond doubt that surface physics in general and physical adsorption in particular promise to be fruitful fields for future research. In view of their growing importance, we wish to review in this article the more relevant papers published on physically adsorbed monolayers and discuss possible interpretations

---

\* Work supported in part by the U.S. National Science Foundation through grants Nos. GP-25306 and GP-11054.

† On leave from Northwestern University, Evanston, Illinois 60201, U.S.A.

(1) J. Low Temp. Phys. 3, 197-337 (1970).

(2) M. Bretz and J.G. Dash, Phys. Rev. Letters 26, 963 (1971).

of recent experimental findings.

### 1. Definition of the Problem

An experiment on physical adsorption begins with the careful preparation of a crystalline surface. This surface must offer a large lateral area so that adsorption can readily take place. Yet it must be microscopically homogeneous to avoid clumping of the adsorbed atoms. Often a sponge-like material is employed as a base, to be sealed off in some insulated cell. A binary mixture of noble gases is then let into the cell. The heavier species will first be adsorbed on the base, forming a smooth coating which in turn serves as the adsorption surface for the lighter atoms. The system of interest then consists of a thin layer of the latter which is in equilibrium with the substrate below and the vapor above. Macroscopic properties which are measurable include heats of adsorption, adsorption isotherms, heat capacities, lateral heat of vaporization, transport coefficients, etc.

A successful theory for adsorbed helium monolayers must undoubtedly be quantum mechanical in nature. One has on hand quantum mechanical many-body systems whose behaviors obey the principles of statistical mechanics. The study of these systems are exceedingly formidable. We shall begin in the present section with the construction of a crude model, followed by a review of some of the relevant experimental facts. In Section II we turn to the quantum mechanical many-body problem and summarize the results of recent theoretical studies. In Section III we focus our attention on the latest experimental findings, report on a number of quantum statistical model calculations, and discuss their relative merits.

A simple picture describing the process of physical adsorption can be given as follows. Consider, for definiteness, a single crystalline substrate in the form of face-centered cubic (fcc) argon. On account of the relatively large mass of the argon atoms we may neglect their zero point motion and assume the argon atoms to be frozen on the lattice sites.<sup>(3)</sup> Such a lattice presents to an incoming helium atom a static, external field, representable by a Morse potential in the direction normal to the surface, and by some periodic potential in the two lateral directions. If the Morse potential is sufficiently deep, the He atom will find itself trapped in the potential well, oscillating about an equilibrium point several Angstroms above the substrate surface. This defines **Physical adsorption**. Depending on the strength of the periodic potential and the degree of thermal agitation, the adsorbed atom, or "adatom", may or may not move freely along the substrate surface. In the two extreme limits we have respectively "mobile" and "localized"

---

(3) See C-W. Woo, J. Low Temp. Phys. **3**, 335 (1970), for suggestions of treatment without this assumption.

adsorptions. As the number of adatoms increases, the interactions between them become important. Consequently dynamical correlations between the adatoms must be brought into consideration. The statistics of the adatoms in principle plays an important role in this quantum mechanical problem. At low coverages, however, statistical effects may be ignored, enabling us to employ classical statistical mechanics. This defines the classical limit which we propose to discuss presently.

## 2. The Classical Limit

In the extreme mobile limit, there is no lateral potential variation so that each adatom is free in the lateral directions. In the normal direction the potential well may be approximated by a harmonic oscillator potential. As a result, the partition function  $q$  for a single adatom is given by

$$q = \frac{\Pi m k T A}{h^2} \sinh(\frac{\hbar \omega}{2kT}), \quad (1)$$

where  $m$  is the mass of the adatom,  $k$  the Boltzmann constant,  $A$  the adsorption area and  $\omega$  the oscillator frequency. For a system of  $N$  adatoms, the partition function is given by the usual formula for independent particles

$$Z = \frac{q^N}{N!}. \quad (2)$$

In the extreme localized limit, each adatom encounters insurmountable potential barriers in the lateral directions. Consequently we may approximate the lateral potential by a sequence of two-dimensional harmonic wells of frequency  $\omega$ . Therefore

$$q = \left[ 8 \sin^2 \left( \frac{\hbar \omega}{2kT} \right) \sinh \left( \frac{\hbar \omega}{2kT} \right) \right]^{-1}, \quad (3)$$

and

$$Z = \binom{M}{N} q^N, \quad (4)$$

where  $M$  denotes the number of adsorption sites. The numerical factors in Eqs. (2) and (4) account for the indistinguishability of the adatoms.

The knowledge of the partition function now enables us to derive from the usual rules of statistical mechanics<sup>(4)</sup> all thermodynamic properties, such as the (two-dimensional) equation of state, heat capacity, etc. In particular, it is easy to find the chemical potential for an adatom. By equating the chemical potentials for the adatoms and the atoms in the vapor, which may in general be approximated as an ideal gas, we obtain the adsorption isotherms. These are curves

---

(4) T.L. Hill, *Introduction to Statistical Thermodynamics*, Addison-Wesley (1960), Chaps. 7 and 14.

on which experimentalists must depend in determining the amount of material adsorbed, as characterized by the areal density:  $\sigma \equiv N/A$ , or the coverage:  $\theta \equiv N/M$ : It is noteworthy that Eqs (2) and (4) lead to specific heats equal to  $2Nk$  and  $3Nk$  respectively in the high temperature limit.

### 3. Recent Experimental Results

During the last several years,<sup>(1)</sup> heat capacity measurements of rare gas monolayers have been carried out by Dash and coworkers at the University of Washington in the United States, and by Brewer's group at the University of Sussex in England. Also, third sound propagation has been studied by Rudnicky at the University of California, Los Angeles, and by Mochel at the University of Illinois, in thin He films thicker than a monolayer. Nuclear magnetic resonance studies are under way at both Washington University and Stevens Institute of Technology. The heat capacity work by Dash and collaborators is at the moment most susceptible to theoretical interpretation. We shall therefore concentrate on their data and briefly review here their recent findings.<sup>(2-4)</sup>

Prior to 1968, Dash, Goodstein and McCormick published a series of papers<sup>(5-7)</sup> on the adsorption isotherms and heat capacities of He<sup>3</sup> and He<sup>4</sup> adsorbed on argon-plated copper sponge. At coverages close to a complete monolayer ( $\theta=1$ ), they found heat capacities quadratic in temperature, signifying the formation of two-dimensional Debye-like solids. At low coverage ( $\theta \ll 1$ ), the heat capacities became linear in temperature, as expected of two dimensional quantum gases. These results were exciting because it appeared that at last physicists have learned how to prepare realistic two-dimensional systems. Theoretical conjectures may now be critically tested in the laboratory.

Between 1968 and 1970, Stewart and Dash carried out more precise measurements of the same nature. Under painstaking scrutiny,<sup>(8-9)</sup> they found that the satisfying and theoretically consistent results obtained previously no longer appeared. At low coverages and low temperatures, if a linear fit to the heat capacity  $C(T)$  was made, it would have to possess a small but negative zero-temperature intercept: clearly an unacceptable conclusion. On the other hand, a quadratic fit would indicate the realization of two-dimensional crystallization at gaseous densities: an equally disturbing implication. It was suggested that somehow the substrate must have played a dominant catalytic role. Either through the application of strong lateral pressures generated by inhomogeneities, or by

(5) D. L. Goodstein, W. D. McCormick and J. G. Dash, Phys. Rev. Letters 15, 447 (1965) ; 15, 740 (1965).

(6) D. L. Goodstein, Ph. D. Thesis, University of Washington (1965).

(7) W. D. McCormick, D. L. Goodstein, and J. G. Dash, Phys. Rev. 168, 249 (1968).

(8) G.A. Stewart and J. G. Dash, Phys. Rev. **A2**, 918 (1970).

(9) G. A. Stewart and J. G. Dash, J. Low Temp. Phys. **3**, 281 (1970).

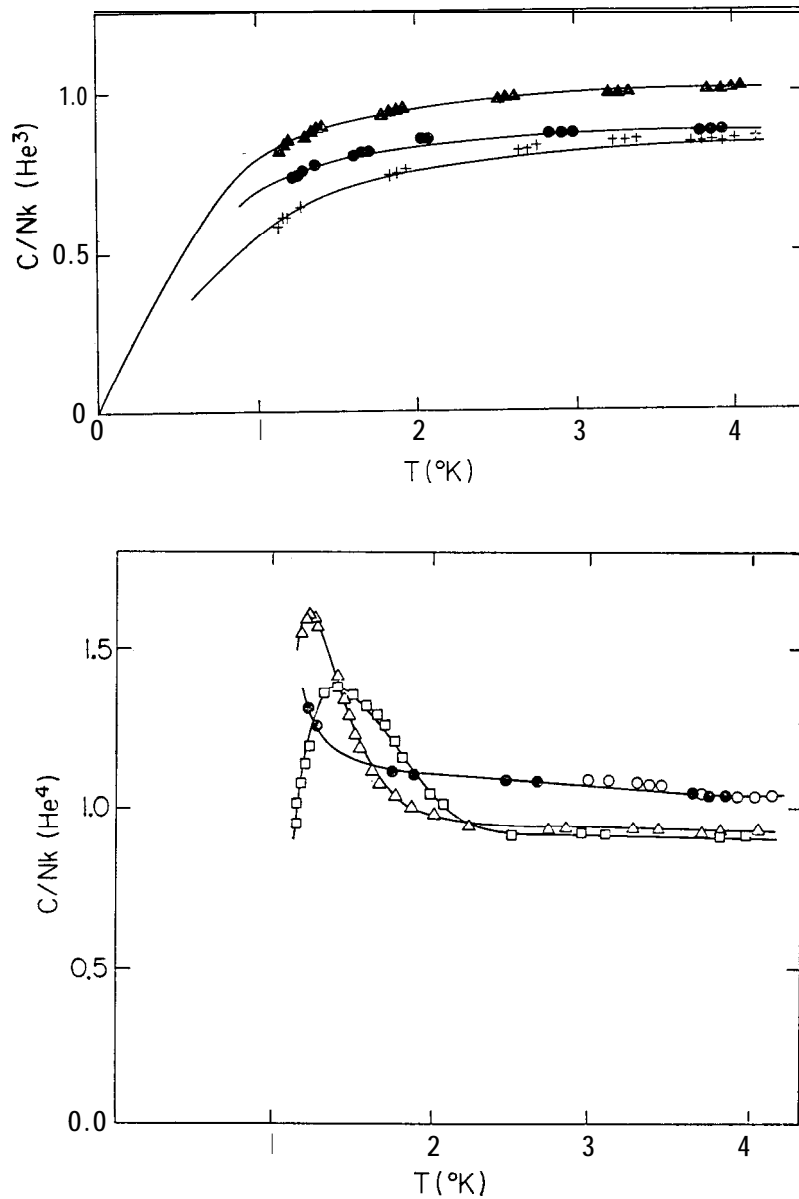


Fig. 1. (a.) Specific heats of  $He^3$  films: closed triangles,  $\theta=0.14$ ; closed circles,  $\theta=0.26$ ; plus signs,  $\theta=0.39$ . Solid curves are fitted theoretical curves for two-dimensional ideal gases.

(b) Specific heats of  $He^4$  films: open circles,  $\theta=0.148$ ; closed circles,  $\theta=0.153$ ; open triangles,  $\theta=0.255$ ; open squares,  $\theta=0.372$ .

Taken from Ref. 27.

mediating extra He-He attraction, the substrate had forced the adatoms to bind into solid patches. We shall return to a more quantitative discussion of this point in Section II.

Substrate inhomogeneities are clearly undesirable complications: they tend to mask the actual properties of the two-dimensional systems under study. Subse-

quently the argon-plated copper substrate was abandoned in favor of graphite, which possesses exceedingly uniform adsorption surfaces. At high temperatures, Bretz and Dash<sup>(2)</sup> found that  $C(T)/Nk$  approached unity for He<sup>4</sup> and He<sup>3</sup> alike, at all coverages. This is consistent with the classical limit for two-dimensional systems. As  $T$  decreased, the He<sup>3</sup> data fell off slowly and smoothly until about 1°K, then turning sharply toward zero as  $T \rightarrow 0^\circ\text{K}$ . Such a temperature dependence can be understood in terms of a Fermi gas model, even though the data seemed to suggest larger Fermi temperatures than can be accounted for. It was the He<sup>4</sup> data which exhibited startling behavior and caused general interest and concern. As  $T$  decreased,  $C(T)$  rose toward a peak in the interval 1–2°K before falling off abruptly near 1° K. (This peak shifted toward lower temperatures and apparently higher magnitudes with decreasing coverage.) Phase transitions were immediately suspected. In fact, we are immediately reminded of the A-transition in liquid He' and Bose gases. However, it is well-known that for a two-dimensional Bose system macroscopic zero-momentum condensation does not occur-unless there exist extenuating conditions. The main body of the present paper will deal in Section III with such conditions.

In Fig. 1 we reproduce for the reader's convenience the specific heat data of Bretz and Dash (Ref. 2).

## II. QUANTUM MECHANICAL CALCULATIONS

We review in this Section existing quantum mechanical calculations dealing with physically adsorbed monolayers. The emphasis will be on recent developments.

The earliest microscopic calculation was that of Lennard-Jones and Devonshire<sup>(10)</sup> in 1932. It involved a separation of the substrate potential, followed by a band-theoretical solution of the Schrödinger equation in the lateral directions. The method was recently shown<sup>(11)</sup> to be inadequate when adapted to study the adsorption of He on A-c, by an extended perturbative calculation. Some ten years ago, Steele and Ross<sup>(12)</sup> approximated the lateral variation of the substrate potential by an infinitely extended V-shape well, and proceeded to calculate the properties of He monolayers at low coverages. Under this approximation the He atoms are trapped at adsorption sites and the lateral motions are automatically ruled out. Recently, Jackson<sup>(13)</sup> investigated the quantum mechanical behavior of He monolayers at full coverage, but his study was limited to the extreme mobile limit. The

---

(10) J. E. Lennard-Jones and A. F. Devonshire, Proc. Roy. Soc. (London) A158, 242 (1932).

(11) H-W. Lai, C-W. Woo and F. Y. Wu, J. Low Temp. Phys. 3, 463 (1970).

(12) W.A. Steele and M. Ross, J. Chem. Phys. 35, 850 (1961); 35, 862 (1961).

(13) H. W. Jackson, Phys. Rev. 180, 184 (1969).

most detailed single particle calculations were those of Ricca, Pisani and Garrone,<sup>(14)</sup> and of Novaco and Milford.<sup>(15)</sup> In both cases, large sets of basis functions were employed to facilitate elaborate numerical calculations. The former authors used atomic orbitals, and the latter simple sinusoidals. Some of the results of these computations are listed in Table 1. A physically more transparent and numerically more tractable procedure which leads to conclusions in general agreement with those of Refs. 14 and 15 has been carried out by the present authors.

Table 1. Numerical results of single particle calculations.  $\epsilon=25.4^\circ\text{K}$  and  $r_0=3.4\text{\AA}$  are used for He-Ar interaction unless otherwise stated. All energies are in " K. The Novaco-Milford (111) results were obtained with a (001) face suitably compressed to simulate the (111) face

	Ricca, Pisani and Garrone <sup>(14)</sup>	Novaco and Milford <sup>(15)</sup>	Lai, Woo and Wu <sup>(11,16)</sup>
<b>Ground State Energy</b>			
He on Kr (001)	-125		-115.0 (Gaussian) -117.9 (Morse) -123.5 (Morse-shift)
He on Ar (001)			- 57.7 (Gaussian) - 58.6 (Morse) - 61.6 (Morse-shift)
He on Ar (031) Using $\epsilon=35^\circ\text{K}$ $r_0=3.35\text{\AA}$		- 9 8 . 6	- 93.5
He on Ar (111)			- 47.3
<b>Band Widths and Gaps</b>			
He on Kr (001)			
1st band width	0.06	0.07	
1st band gap	38	33	
2nd band width	1.8	3.0	
He on Ar (001)			
1st band width		0.1	0.09
1st band gap		38	34
2nd band width		3.0	1.9
He on Ar (111)			
1st band width		( 4.9)	4.9
1st band gap		(24.4)	22
2nd band width		(20.4)	26

(14) F. Ricca, C. Pisani and E. Garrone, J. Chem. Phys. 51, 4079 (1969).

(15) A. D. Novaco and F. J. Milford, J. Low Temp. Phys. 3, 307 (1970).

(11-16) This procedure is now briefly reviewed.

### 1. The Many Particle Hamiltonian

For  $N$  He atoms adsorbed on a crystalline surface, e. g., a **(001)** or (111) face, of fcc argon, the Hamiltonian can be written as:

$$H = \sum_{i=1}^N \frac{-\hbar^2}{2m} \nabla_i^2 + \sum_{i=1}^N \mathcal{V}(\mathbf{r}_i) + \sum_{i < j=1}^N v(\mathbf{r}_{ij}), \quad (5)$$

where  $v(\mathbf{r})$  denotes the He-He interaction, well approximated by the Lennard-Jones 6-12 potential

$$v(\mathbf{r}) = \epsilon \left[ \left( \frac{r_0}{r} \right)^{12} - 2 \left( \frac{r_0}{r} \right)^6 \right], \quad (6)$$

with<sup>(17)</sup>  $\epsilon = 10.22^\circ\text{K}$  and  $r_0 = 2.89\text{\AA}$ .  $\mathcal{V}(\mathbf{r})$  is a single particle function which represents the substrate potential: the field due to all the argon atoms acting on a He atom at the field point  $\mathbf{r}$ . Let  $\mathbf{V}(\mathbf{r})$  denote the He-Ar potential, also in the Lennard-Jones 6-12 form, with  $\epsilon = 25.4^\circ\text{K}$  and  $r_0 = 3.4\text{\AA}$ .  $\mathcal{V}(\mathbf{r})$  is then given by the lattice summation

$$\mathcal{V}(\mathbf{r}) = \sum_{\alpha} V(|\mathbf{r} - \mathbf{r}_{\alpha}|) \approx \sum V(|\mathbf{r} - \mathbf{R}_{\alpha}|), \quad (7)$$

where  $\alpha$  runs over all Ar atoms in the substrate lattice and  $\mathbf{R}_{\alpha}$  denotes the lattice vectors. The evaluation of lattice sums requires nothing more than conventional

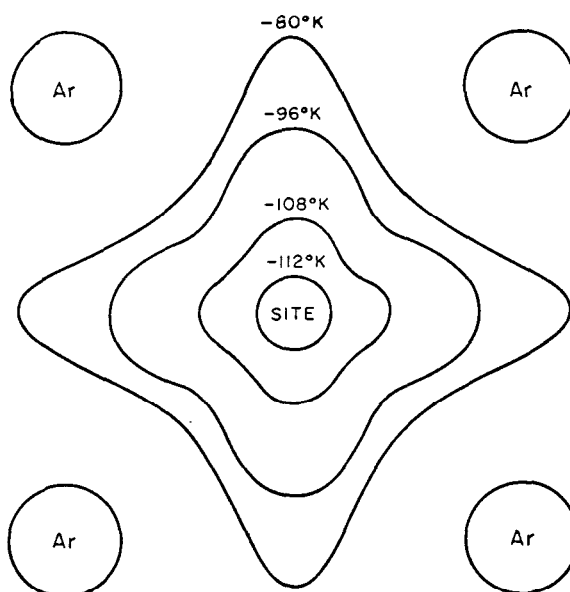


Fig. 2. The equipotential contours of the fcc argon substrate potential in the  $z=2.44\text{\AA}$  plane of the (001) face. Taken from Ref. 16.

(16) H-W. Lai, C-W. Woo and F. Y. Wu, J. Low Temp. Phys. Vol. 5, No. 5 (1971).

(17) All energies will be measured in units of the Boltzmann constant  $k$ .

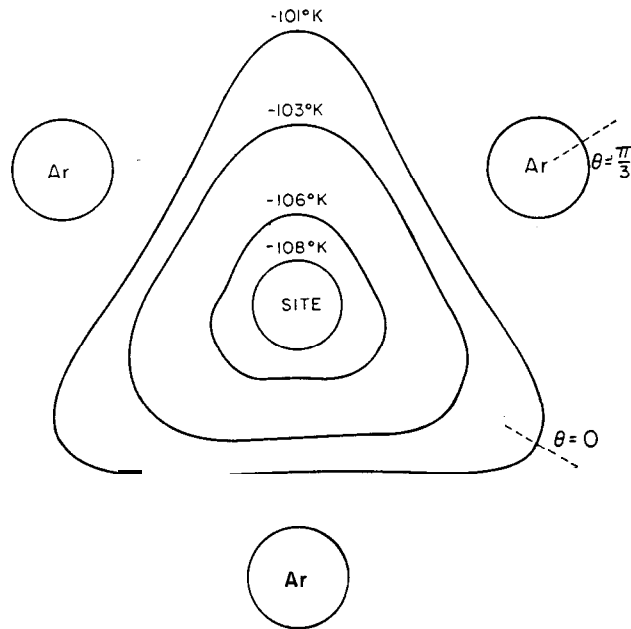


Fig. 3. The equipotential contours of the fcc argon substrate potential in the  $z=2.88\text{\AA}$  plane of the (111) face. Taken from Ref.

techniques and machine computations, and results in potential contours like those shown in Figs. 2 and 3, for respectively the (001) face and the (111) face of fcc argon.

## 2. Ground State Variational Calculation in the $\theta \rightarrow 0$ Limit

In the zero coverage limit we may neglect the third term in the Hamiltonian Es. (5) and thus reduce to a one-body problem. The lateral variation of the substrate potential suggests that a close approximation to the single particle ground state wavefunction can be found in the form of a Gaussian.<sup>(11)</sup> In other words, a Gaussian function:

$$\begin{cases} G(\mathbf{r}|a, a') \equiv G(x|a)G(y|a)G(z|a'), \\ G(x|a) \equiv \frac{1}{\pi^{1/4}} e^{-\frac{1}{2}a^2x^2} \end{cases} \quad (8)$$

repeated over all adsorption sites, serves well as a trial wavefunction in finding the ground state energy  $e_0$  of the single particle Schrödinger equation

$$h\varphi_0(\mathbf{r}) = e_0\varphi_0(\mathbf{r}),$$

where

$$h = \frac{-\hbar^2}{2m} \nabla^2 + \psi(\mathbf{r}). \quad (10)$$

The energy can be lowered further (by a few percent) if in the normal direction

we replace the Gaussian  $G(\mathbf{z}|\mathbf{a}')$  by a Morse function:(“ )

$$\begin{cases} M(\mathbf{z}|\kappa, \beta, \delta) = [\kappa(2\delta-1)/\Gamma(2\delta)]^{1/2} e^{i\pi(2\delta-1)-1} z w^{1/2(2\delta-1)}. \\ w = 2\delta e^{-\kappa(z-\beta)}. \end{cases} \quad (11)$$

Finally, the best result is obtained by (i) allowing the peak of the Morse function to shift toward (or away from) the substrate surface when  $(x, y)$  drifts toward the center (or boundary) of an adsorption site, and (ii) taking into account the symmetry of the substrate<sup>(16)</sup> by varying the width  $\alpha^{-1}$  of the Gaussian with the angle  $\varphi \equiv \arctan(y/x)$ .

Numerical results of these variational computations are displayed in Table 1.

### 3. Bandwidths

As an adatom travels away from the center of an adsorption site, it encounters periodic lateral variations of the substrate potential. The amplitude of these variations depends on  $\mathbf{z}$  as well as the angle  $\varphi$ . Averaging over all  $\mathbf{z}$  and  $\varphi$ , using the ground state wavefunction (or rather its square-the probability) as a weighting factor, we find<sup>(16)</sup> the resulting potential  $\bar{V}$  roughly sinusoidal in the variable  $\rho \equiv (x^2 + y^2)^{1/2}$ . The Schrödinger equation

$$\left[ \frac{-\hbar^2}{2m} \frac{\partial^2}{\partial \rho^2} + \bar{V}(\rho) \right] \chi(\rho) = E \chi(\rho) \quad (12)$$

then governs the lateral motion of the He atom. Its solutions are in the form of Mathieu functions,<sup>(19)</sup> corresponding to eigenvalues forming a band spectrum. We thus obtain band widths and band gaps which may be regarded as parameters characterizing the lateral mobility of the adatoms. Some of our numerical results are included in Table 1. Note that the close-packed (111) face is smoother than the (001) face, permitting greater freedom in lateral motion, as reflected in the much larger band widths calculated.

### 4. Correlation Energy

Returning to the many particle Hamiltonian, Eq. (5), we now investigate the variational calculation for He monolayers at finite coverages. Let  $\psi(\mathbf{r}_1, \mathbf{r}_2, \dots, \mathbf{r}_N)$  denote a trial wavefunction; an upper bound of the ground state energy  $E_0$  of the system is

$$E[\psi] \equiv \langle \psi | H | \psi \rangle / \langle \psi | \psi \rangle. \quad (13)$$

On account of the repulsive core in the 6-12 potential, we cannot simply take as a trial wavefunction the properly symmetrized (denoted by  $\mathcal{P}$ ) product of

(18) The direction normal to the substrate surface is designated as the z-direction.

(19) *Handbook of Mathematical Functions*, eds. M. Abramowitz and I. A. Stegun, National Bureau of Standards, Wash., D. C. (1964), section 20.

single particle functions

$$\varphi(\mathbf{r}_1, \mathbf{r}_2, \dots, \mathbf{r}_N) \equiv P \left\{ \prod_{i=1}^N \varphi_0(\mathbf{r}_i) \right\}; \quad (14)$$

the energy integral would diverge as a result of single particle wavefunctions overlapping each other's repulsive region. A correlating factor must be introduced to distort the wavefunctions at their mutual approach. A convenient and well-tested form of the correlating factor is the Jastrow function

$$F(\mathbf{r}_1, \mathbf{r}_2, \dots, \mathbf{r}_N) \equiv \prod_{i < j=1}^N f(\mathbf{r}_{ij}), \quad (15)$$

where the two-particle function  $f(r)$  decays rapidly as  $r \rightarrow 0$ . Using

$$\psi = F\varphi, \quad (16)$$

the energy expectation value  $E[\psi]$  becomes now a many-body integral, which can be approximately evaluated by techniques borrowed from the theory of classical liquids, such as solving integral equations for distribution functions, cluster expansion methods, and molecular dynamics. At low coverages we find<sup>(16)</sup> for He'

$$E[\psi] = E^{(0)} + \theta E^{(1)} + O(\theta)^2, \quad (17)$$

where

$$E^{(0)} = Ne_0, \quad (18)$$

and

$$\begin{aligned} E^{(1)} = & \frac{\theta}{2} \int \varphi_0^2(\mathbf{r}_1) \varphi_0^2(\mathbf{r}_2) f^2(\mathbf{r}_{12}) \left[ v(\mathbf{r}_{12}) - \frac{\hbar^2}{2m} \nabla_{12}^2 \ln f(\mathbf{r}_{12}) \right] d\mathbf{r}_1 d\mathbf{r}_2 \\ & + N \left\{ \int_s \varphi_0^2(\mathbf{r}) A(\mathbf{r}) \mathcal{V}(\mathbf{r}) d\mathbf{r} + \frac{\hbar^2}{2m} \int_s [\nabla \varphi_0(\mathbf{r})]^2 A(\mathbf{r}) d\mathbf{r} \right. \\ & \left. - \frac{\hbar^2}{4m} \int_s \varphi_0(\mathbf{r}) \nabla \varphi_0(\mathbf{r}) \cdot \nabla v(\mathbf{r}) d\mathbf{r} \right\}, \end{aligned} \quad (19)$$

with

$$A(\mathbf{r}) \equiv \int \varphi_0^2(\mathbf{r}') [f^2(|\mathbf{r}-\mathbf{r}'|) - 1] d\mathbf{r}'. \quad (20)$$

The symbol  $\int_s$  denotes integration over the extent of an adsorption site, while  $\int$  denotes integration over all space.

Taking  $f(r)$  to be a step function which rises abruptly from 0 to 1, at  $r = 0.5\text{\AA}$ , we find

$$\theta E^{(1)} \approx -1.6N^\circ\text{K}. \quad (21)$$

It is convenient to define a correlation energy  $e_c$  as

$$e_c = \frac{E_0}{N} - e_0. \quad (22)$$

Equations (17), (18), (21) and (22) then yield

$$e_c \leq -1.6^\circ\text{K}. \quad (23)$$

### 5. Surface Phonons

Assuming that we are able to obtain the complete set of eigenfunctions  $\varphi_n(\mathbf{r})$  of Eq. (9), the model function  $\varphi$  of Es. (14) can be generalized to obtain a complete set of many-particle functions

$$\varphi_{n_1 n_2 \dots n_N}(\mathbf{r}_1, \mathbf{r}_2, \dots, \mathbf{r}_N) \equiv P \left\{ \prod_{i=1}^N \varphi_{n_i}(\mathbf{r}_i) \right\}, \quad (24)$$

giving rise to a set of correlated basis functions

$$\psi_{n_1 n_2 \dots n_N}(\mathbf{r}_1, \mathbf{r}_2, \dots, \mathbf{r}_N) \equiv F \varphi_{n_1 n_2 \dots n_N}(\mathbf{r}_1, \mathbf{r}_2, \dots, \mathbf{r}_N). \quad (25)$$

It can be shown<sup>(11)</sup> that these  $\psi$ 's are precisely the unperturbed surface phonon functions (surf ons) of Jackson.<sup>(13)</sup> We thus have on hand a natural starting point for studying the collective excitations which exist and propagate in physically adsorbed He monolayers.

### 6. Contact with **Experiment**

The microscopic calculations described in the present Section were carried out with purpose of obtaining some order-of-magnitude estimates, to enable theorists making contact with experiment. For example, the ground state variational calculation leads to an estimate of the heat of adsorption. It must be emphasized that any search for detailed agreement will prove to be futile, for realistic experimental substrates can hardly be simulated by perfect single crystals. Nevertheless, numerical results indicate that He atoms are more tightly bound on a (001) face than on a (111) face, and that the binding energy is of the order of  $50^\circ\text{K}$ , which suggests that desorption is not significant at the experimental temperatures (1–4 $^\circ\text{K}$ ). These are informations useful for the experimentalists.

Novaco and Milford<sup>(20)</sup> have recently extended their single particle computations to graphite substrates. They found the substrate potential-well in the normal direction much deeper and narrower than that for argon. This means tighter binding and more restricted motion in the normal direction, permitting the formation of a more realistic two-dimensional system. They also found that the

---

(20) A. D. Novaco and F. J. Milford, preprint.

excitation energy in the  $z$  direction amounts to some  $80^\circ\text{K}$ , which means that at low temperature, as far as the normal direction is concerned, the adsorbed atoms will always remain in their nodeless, Gaussian-like, ground state. Under such circumstances, all the measurable thermodynamic properties result from lateral motions. This casts the determination of band widths and band gaps in the spotlight of attention.

The band structure calculation contributes significantly towards understanding experimental data. Let us illustrate this with a concrete example. On the (001) face of argon, the first band width is only  $0.1^\circ\text{K}$ . This indicates extremely sluggish lateral motion. Each adsorbed atom is confined to its site, and is permitted to do little more than oscillating in a three-dimensional well. The situation corresponds to the localized limit discussed in Section I. 2. Consequently the heat capacity is expected to behave like that of an Einstein solid: essentially exponential at low temperatures. Such behavior is qualitatively unchanged even when the areal density increases toward full coverage. Correlation effects are relatively unimportant. On the other hand, on the (111) face of argon, the first band width is some 50 times larger, meaning that the atoms are much more mobile. Correlation effects will actually dominate, allowing the atoms to interact strongly with one another. As the areal density or coverage is increased, the adsorbed atoms form two-dimensional solids, giving rise to  $T^2$  specific heats, which were apparently observed experimentally. For graphite, Novaco and Milford<sup>(20)</sup> found that the band widths are even larger: the bands actually overlap. The atoms are practically free in the lateral directions. This situation corresponds then to the mobile limit discussed in Section I. 2.

The correlation energy computed is also of some interest. On the (001) face, each atom has 4 nearest neighbors, giving rise to a total of  $4 \times (-1.6) = -6.4^\circ\text{K}$  of lateral binding. This number will yet be lowered by second order perturbative corrections and by binding to next nearest neighbors. Stewart and Dash<sup>(9)</sup> reported a lateral heat of vaporization of some  $15^\circ\text{K}$ , not inconsistent with our crude theoretical estimate. Better agreement may yet be found if one employs the fact that the argon plating on copper resembles a (111) face of the single crystal, and that the correlation energy may yet turn out to be more negative on the (111) face. However, such a calculation requires an accurate determination of the correlating factor  $f(r)$ . The latter is as yet unavailable.

### III. STATISTICAL MECHANICAL MODEL CALCULATIONS

Having reviewed the general theory of physical adsorption and presented results of recent quantum mechanical calculations, we now turn our attention to

statistical mechanics. The thermodynamics of a given system may be derived from the canonical partition function  $Z$  or the grand partition function  $\Xi$ . These functions are in principle straightforward to compute, provided that we could find an exact solution to the quantum mechanical problem defined in Section II. Unfortunately the latter is not accessible. As is usual in statistical mechanics, we are forced to consider model systems.

We must point out that it is very difficult to decide *a priori* which model to use, for at the present stage the physical mechanism of adsorption remains unclear. In fact, it is our hope that, through model studies and comparison with experiments, we could attain better understanding of some of the basic features of adsorption. With this goal in mind, we shall construct in the present Section a number of reasonable models and compare theoretical results with recent data on heat capacities, ( ) as given in Fig. 1.

Let us first summarize the standard procedure for computing thermodynamic quantities in quantum statistical mechanics for a non-interacting many-particle system. ( ) Assuming the single particle energy spectrum  $\{E\}$  known, in the grand canonical ensemble one first computes the fugacity  $z$  from

$$N = \sum_{\epsilon} \frac{1}{z^{-1}e^{\beta\epsilon} \pm 1}. \quad (26)$$

The grand partition function  $\Xi$  is then given by

$$\ln \Xi = \pm \sum_{\epsilon} \ln(1 \pm ze^{-\beta\epsilon}). \quad (27)$$

thermodynamic quantities follow from Eq. (27). For example, the energy per particle is given by

$$e = \lim_{N \rightarrow \infty} \frac{E}{N} = - \frac{\partial}{\partial \beta} \lim_{N \rightarrow \infty} \frac{1}{N} \ln \Xi \Big|_{z = \text{constant}} \quad (28)$$

In Eqs. (26) and (27), and all equations to follow, the upper (lower) sign is used for a Fermi (Bose) system, also  $\beta = 1/kT$ . It is also important to take the thermodynamic limit  $N \rightarrow \infty$  in, e. g., Eq. (28), before one computes derivatives. Finally, we shall, in the following, consider spinless fermions and bosons and bosons. In the case of nonzero spins, the only change required is to associate a spin degeneracy factor with each of the extensive quantities.

### 1. Two-Dimensional Ideal Gas

If the substrate potential has weak lateral (periodic) variations, we expect the adatoms at low coverages to behave like a two-dimensional ideal gas. It is well-known that the two-dimensional ideal Bose gas, unlike its three-dimensional

---

(21) See, for example, K. Huang, *Statistical Mechanics* (Wiley), Chap. 9.

counterpart, does not undergo Bose-Einstein condensation. In fact, it can be shown<sup>(22)</sup> that the specific heats for two-dimensional Fermi and Bose gases are identical. This fact is inconsistent with the data shown in Fig. 1. Consequently the two-dimensional ideal gas model is immediately ruled out by experiment. For purposes of orientation, it would be useful to discuss this, the simplest of all models, even though it does not fit the data.

The two-dimensional ideal gas was studied by May.<sup>(22)</sup> Using a mathematical identity, he was able to show that the series expansions for the fermion and boson energies,  $e_F$  and  $e_B$ , given by Eq. (28) are related by

$$e_F = e_B + \frac{1}{2}kT_0, \quad (29)$$

where  $T_0$  is the temperature at which the thermal wavelength  $\lambda = h/(2\pi mkT)^{1/2}$  equals the average atomic spacing

$$\frac{1}{\sigma} = \lambda_0^2 = \frac{h^2}{2\pi mkT_0} \quad (30)$$

and  $\sigma$  is the areal density defined at the end of Section I. 2. The proof given by May is not strictly correct, for the series expansion he introduced (Eq. (13) of Ref. 22) does not converge for  $|z| > 1$ . His conclusion is nevertheless correct and can be simply obtained as follows.<sup>(23)</sup>

For a two-dimensional ideal gas we replace  $\sum_{\epsilon}$  in Eq. (26) by the integral  $\frac{A}{(2\pi)^2} \int dk, dk$ , and obtain the chemical potential

$$\mu = kT \ln z = kT \ln |e^{\pm \lambda^2 N/A} - 1|. \quad (31)$$

The Helmholtz free energies  $F_F$  and  $F_B$  can next be computed from the identity

$$F = \int_0^N \mu dN. \quad (32)$$

It is then a simple matter to verify from Eqs. (31) and (32) that

$$F_F = F_B + \frac{1}{2}NkT_0. \quad (33)$$

Equation (29) then follows from the relation  $e = \frac{\partial}{\partial \beta}(\beta F)$ . The specific heat can now be computed and is seen to be identical for Fermi and Bose gases (See Fig. 4 below).

(22) R. M. May, Phys. Rev. 6, A1515 (1964).

(23) This derivation is due to A. Widom.

## 2. Ideal Gas with Two Energy Levels in the Normal Direction.

In the two-dimensional ideal gas model considered above, the adatoms are confined to move only in lateral directions. An immediate modification of the above model calls for the relaxation of this constraint. The substrate is now considered as providing a potential well of finite width and depth, in the normal direction. We further assume that, in the temperature range of interest, only the two lowest bound states in this potential well are of significance. Let  $A$  be the spacing between the two energy levels and designate the lower one to be of zero energy. Equation (26) now leads to

$$\sigma = \pm \lambda^2 [\ln(1 \pm z) + \ln(1 \pm ze^{-\beta A})]. \quad (34)$$

Solving  $z$  from Eq. (34), we obtain

$$z = \frac{1}{2} \left\{ \pm (e^{\beta A} + 1) \mp [(e^{\beta A} - 1)^2 + 4e^{\beta A + 1/2} \lambda^2]^{1/2} \right\} \quad (35)$$

Combining Eqs. (27), (28), and (35), we find the energy  $\epsilon$  most conveniently expressed in terms of the functions

$$g_n(x) = \sum_{m=1}^{\infty} \frac{x^m}{m^n} \quad (36)$$

and

$$f_n(x) = -g_n(-x).$$

After some straightforward but lengthy algebraic steps, we obtain the following expression for the specific heat per adatom:

Bosons :

$$C_B = \frac{\Delta}{T_0} \left[ \frac{\beta \Delta - y}{z^{-1} e^{\beta A} - 1} - 2 \ln(1 - ze^{-\beta A}) - \frac{T_0}{\Delta} y + 2g_2(z) + 2g_2(ze^{-\beta A}) \right] \quad (37a)$$

Fermions :

$$\begin{aligned} C_F &= \frac{\Delta}{T_0} \left[ B_1 - \frac{T_0}{\Delta} y + A_1 \right], & z < 1 \\ &= \frac{\Delta}{T_0} \left[ B_2 - \frac{T_0}{\Delta} y + A_2 \right], & 1 < z < e^{\beta A} \\ &= \frac{\Delta}{T_0} \left[ B_3 - \frac{T_0}{\Delta} y + A_3 \right], & z > e^{\beta A} \end{aligned} \quad (37b)$$

where

$$A_1 = 2f_2(z) + 2f_2(ze^{-\beta A})$$

$$\begin{aligned}
 A_2 &= \frac{\pi^2}{3} + (\ln z)^2 - 2f_2(z^{-1}) + 2f_2(ze^{-\beta\Delta}), \\
 A_3 &= \frac{2\pi^2}{3} + 2(\ln z)^2 - 2f_2(z^{-1}) - 2f_2(z^{-1}e^{\beta\Delta}), \\
 B_1 &= B_2 = 2 \frac{\Delta - y}{z^{-1}e^{\beta\Delta} + 1}, \\
 B_3 &= -2 \frac{y + \Delta}{z^{-1}e^{\beta\Delta} + 1},
 \end{aligned}$$

and

$$y = \frac{\beta}{z} \frac{dz}{d\beta} \text{ in all expressions.}$$

As  $T \rightarrow \infty$ , we find  $C \rightarrow k$ , as expected of a two-dimensional gas. On the other hand, in the  $T \rightarrow 0$  limit we find

$$C_B = \frac{\pi^2 k T}{3 T_0} \quad (38a)$$

$$\begin{aligned}
 C_F &= \frac{\pi^2 k T}{3 T_0}, & \Delta > k T_0 \\
 &= \frac{2\pi^2 k T}{3 T_0}, & \Delta < k T_0
 \end{aligned} \quad (38b)$$

Equation (38b) is easy to understand on physical grounds. We note that  $kT_0 = \hbar^2 \sigma / 2\pi m$  is just the Fermi energy. Therefore for  $\Delta > kT_0$  the higher of the two energy levels is not occupied at  $T=0$ . One has essentially a one-level system ( $\Delta = \infty$ ) for which  $C_F = C_B$ . For  $\Delta < kT_0$ , however, both levels are occupied. Consequently the density of states at the Fermi level doubles, and so does the specific heat. In the limit of  $\Delta \rightarrow \infty$ , the case of ideal two-dimensional gas, one recovers the result that  $C_B$  and  $C_F$  are identical, using the mathematical identity given by May.<sup>(22)</sup>

We have numerically evaluated  $C_B$  and  $C_F$  using Eq. (37). The results are presented in Fig. 4. The Fermi and Bose systems behave in a similar manner, each exhibiting a peak. For  $\text{He}^4$ , the location and height, as well as the coverage dependence, of this peak can be fitted quite well to experiment (Fig. 1) by choosing an appropriate  $A$ . It is however clear that the model fails to describe the fermion data. Also, the value of  $A$  for  $\text{He}^4$  appears to be an order of magnitude smaller than what one expects from results of single particle calculations<sup>(20)</sup> based on a reasonable fit of the actual potential well in the normal direction.

### 3. Ideal Gas with One Bound State

From considering the models described above, we realize that the principal difficulty in constructing a valid model lies in explaining the peak which exists in

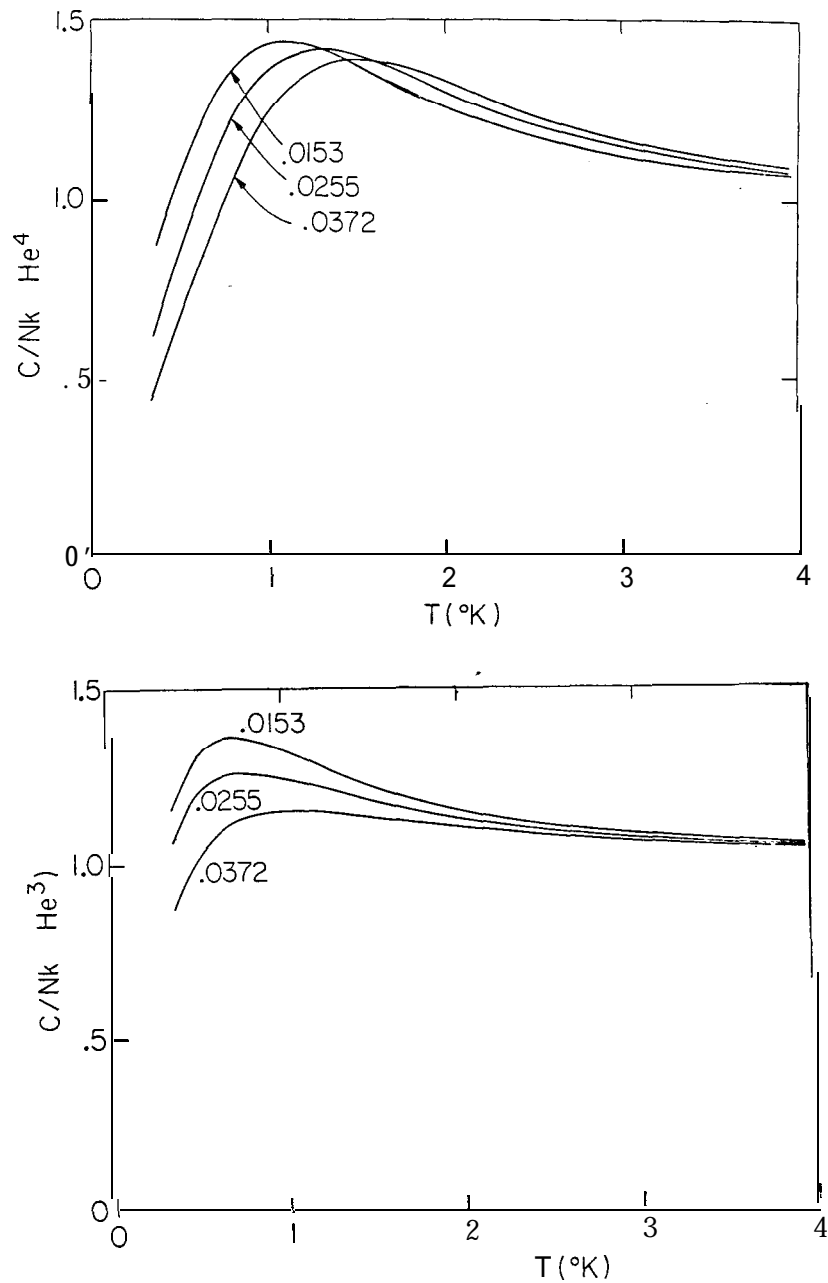


Fig. 4. The specific heats for two-dimensional ideal gases with two energy levels in the normal direction. (a) Bosons (b) Fermions. In both cases  $\Delta=2.0^{\circ}K$ .

the specific heat of the Bose system but not in the Fermi system. One model which possesses this feature will now be discussed.

So far in all the models considered we have permitted the adatoms to move freely in the lateral directions. Suppose we now relax this condition and assume the existence of lateral potential wells capable of trapping the adatoms. If the potential wells are sparsely distributed such that the number of potential traps is

much smaller than the number of adatoms, there will be few adatoms trapped in the fermion case because of the exclusion principle. The system then behaves like the two-dimensional ideal Fermi gas, with no peak in the specific heat. In the boson case, however, it is possible to pile up a large number of particles in any local potential well, resulting in Bose-Einstein condensation and an anomaly in the specific heat. This model is not inconsistent with the recently proved rigorous result<sup>(24,25)</sup> that Bose-Einstein condensation is forbidden in two-dimensions as long as the particle density is everywhere bounded. For it is clear that in the present model the areal density around a potential well is unbounded in the thermodynamic limit.

For simplicity we shall assume the existence of just one bound state in each local potential well and let  $\Delta$  denote the gap between the bound state and the continuum. For fermions, the effect of the bound state is negligible and one has an ideal Fermi gas. For bosons, however, one must single out the terms in (26) and (27) contributed by the bound state and proceed with care. We obtain

$$\sigma = \frac{\sigma}{N} \frac{1}{z^{-1}e^{-\beta\Delta} - 1} - \lambda^{-2} \ln(1-z) \quad (39)$$

and

$$\frac{1}{N} \ln \Xi = -\frac{1}{N} \ln(1 - ze^{\beta\Delta}) - \frac{1}{\sigma\lambda^2} g_2(z). \quad (40)$$

We see that macroscopic occupation of the bound state occurs when  $z = e^{-\beta\Delta}[1 - O(1/N)]$ . This leads to a Bose-Einstein condensation at a temperature  $T_c$  defined by

$$\sigma = -\lambda_c^{-2} \ln(1 - e^{-\beta_c\Delta}). \quad (41)$$

We further find:

$$\frac{1}{N} \ln \Xi \cong -\frac{1}{\sigma\lambda^2} g_2(z), \quad (40a)$$

$$T > T_c: \quad z = 1 - e^{-T_0/T}$$

$$C_B = \frac{2kT}{T_0} g_2(z) - \frac{\beta}{z} \frac{dz}{d\beta}, \quad (42a)$$

$$T < T_c: \quad z = 1$$

$$C_B = \frac{2kT}{T_0} g_2(e^{-\beta\Delta}) - \frac{\Delta}{T_0} \ln(1 - e^{-\beta\Delta}) \quad (42b)$$

(24) J. J. Rehr and N. D. Mermin, Phys. Rev. **B1**, 3160 (1970).

(25) J. F. Fernandez, to be published in the Phys. Rev.

$$\sigma_0 = \sigma \left[ 1 + \frac{T}{T_0} \ln(1 - e^{-\beta \Delta}) \right]$$

where  $\sigma_0$  is the areal density of particles in the condensate. We plot in Fig. 5 numerical results on  $C_B$  for some typical values of  $\Delta$  and  $\sigma$ . The discontinuity of  $C_B$  at  $T_c$  can be traced to the fact that  $\frac{dz}{d\beta}$  is discontinuous at  $T_c$ . Note that in three dimensions  $\frac{dz}{d\beta}$  is continuous since  $\left(\frac{dz}{d\beta}\right)_{T_c+} \propto 1/g_{1/2}(1) = 0$ . Therefore we have in that case a continuous specific heat.

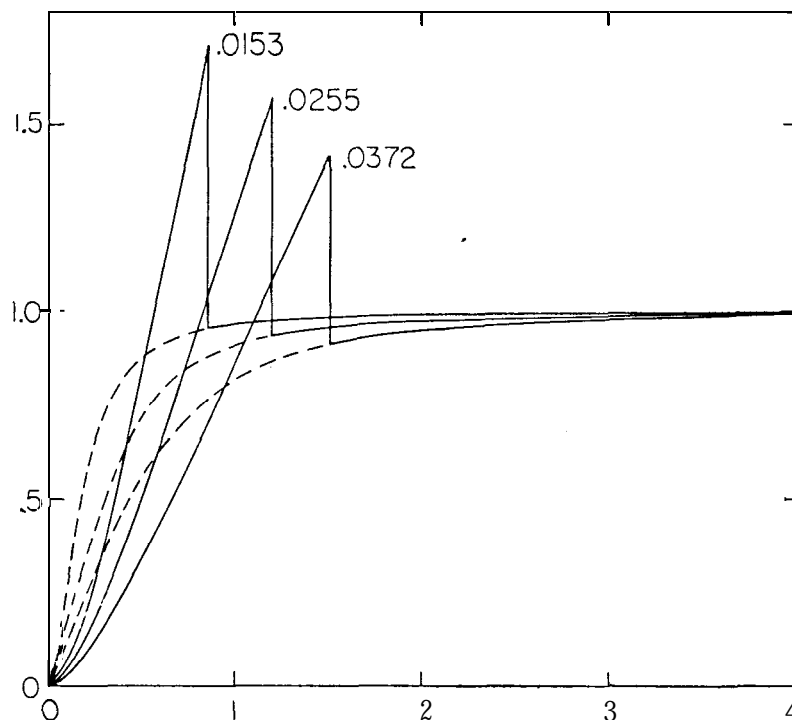


Fig. 5. The specific heats for two-dimensional ideal gases with a single particle bound state. Solid curves: bosons (mass 4) with  $\Delta=0.26^\circ\text{K}$ , dashed curves: free fermions (mass 4).

Comparing our numerical results to experimental data, it appears that the fit in the boson case is not altogether acceptable. On the other hand, the interactions between the adatoms may have the effect of softening the spikes. The interpretation offered here may yet be salvageable.

#### 4. Two-Dimensional Tunneling Model

On the substrate surface of a perfect crystal, the adatoms move in a laterally periodic potential. As a result, the single particle has an energy band spectrum. Mobility of the adatoms arises from tunneling between neighboring adsorption

sites. This forms the basis of the "tunneling model"<sup>(26)</sup> which we now describe.

The simplest band structure, as assumed by Dash and Bretz,<sup>(26)</sup> consists of a zero-point tunneling band of width  $6$ , and an upper, infinitely extended, thermal conduction band separated from the tunneling band by an energy gap  $A$  (see Fig. 6). For  $\delta=0$  this model reduces to the bound state model proposed in the previous subsection, for which a Bose-Einstein condensation occurs in the boson case. For,  $\delta \neq 0$  Bose-Einstein condensation will not occur, as is evident from the fact that the integral in Eq. (26) diverges at  $z=1$ . Nevertheless there will be some remnants of the specific heat anomaly, appearing in the form of a smooth, finite peak. In Fig. 7 we show some typical results of numerical calculations.<sup>(26)</sup> The Fermi and Bose systems behave similarly under this description.

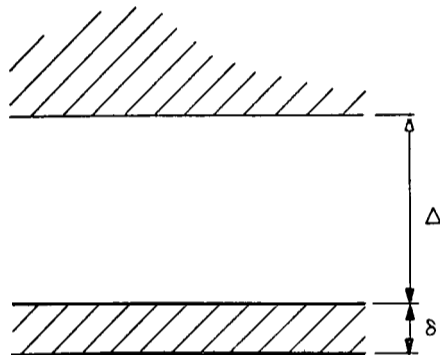


Fig. 6. Energy level diagram for the tunneling model.

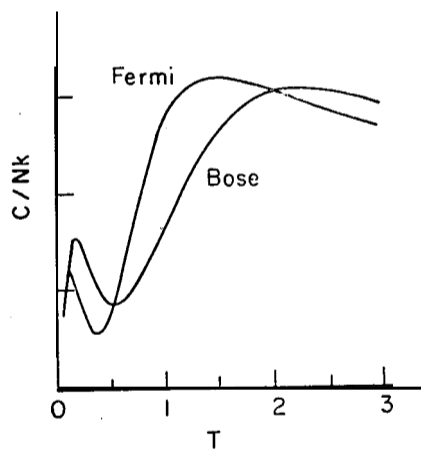


Fig. 7. Comparison of specific heats of the tunneling model at coverage  $\theta=0.5$  and interband gap  $\Delta=2\delta$ ,  $T$  is measured in units of  $\delta/k$ .  
(Take from Ref. 26)

(26) J.G. Dash and M. Bretz, Phys. Rev. 174, 247 (1968).

(27) C. E. Campbell, J. G. Dash and M. Schick, Phys. Rev. Letters 26, 966 (1971).

### 5. Inhomogeneous Substrate Field

Campbell, Dash and Schick<sup>(27)</sup> attributed the observed anomaly in the heat capacity of He<sup>4</sup> monolayers to the assumed presence of an inhomogeneous substrate field. We now present their arguments from a somewhat different point of view.<sup>(28)</sup>

In the presence of an inhomogeneous substrate, the total energy of a single particle becomes  $\frac{p^2}{2m} + E$ , where  $E$  denotes the binding energy or heat of adsorption with a probabilistic distribution  $g(E)$ . Let

$$\int_0^\infty g(E) dE = 1 \quad (43)$$

where we have taken the lower limit of the binding energy to be the zero level. Then Eqs. (26) and (27) become

$$\sigma = \frac{\sigma/N}{z^{-1} \pm 1} + \frac{1}{h^2} \int_0^\infty g(E) dE \int_0^\infty \frac{2\pi p dp}{z^{-1} e^{\beta \frac{p^2}{2m} + \beta E} \pm 1} \quad (44a)$$

and

$$\frac{1}{N} \ln \Xi = \pm \frac{1}{N} \ln(1 \pm z) \pm \frac{1}{h^2} \int_0^\infty g(E) dE \int_0^\infty 2\pi p dp \ln \left( 1 - z e^{-\beta \left( \frac{p^2}{2m} + E \right)} \right) \quad (44b)$$

In Eq.(44) we have separated out the term corresponding to zero energy. This term contributes only in the boson case and leads to Bose-Einstein condensation.<sup>(29)</sup>

The model considered in Ref. 28 corresponds to the following choice of  $g(E)$  :

$$\begin{aligned} g(E) &= \frac{1}{\Delta}, & 0 < E < \Delta \\ &= 0, & \text{otherwise.} \end{aligned} \quad (45)$$

With this simple expression of  $g(E)$ , the integrals in Eq. (44) can be performed and we obtain the following:

$$\begin{aligned} C_F &= \frac{k^2 T}{\lambda^2 \sigma \Delta} \left\{ 6f_3(z) - 6f_3(ze^{-\beta \Delta}) - 4\beta \Delta f_2(ze^{-\beta \Delta}) - \beta^2 \Delta^2 f_1(ze^{-\beta \Delta}) \right. \\ &\quad \left. - \frac{[2\sigma \lambda^2 - f_1(ze^{-\beta \Delta})]^2}{f_1(z) - f_1(ze^{-\beta \Delta})} (\beta \Delta)^2 \right\} \end{aligned} \quad (46a)$$

$$C_B = \text{Eq. (46a) with } f_n \text{ replaced by } g, \quad T > T_c \quad (46b)$$

(28) One of us (FYW) is indebted to Prof. A. Widom for calling his attention to this alternate interpretation.

(29) The additional energy distribution  $g(E)dE$  is equivalent to adding one more degree of freedom to the particle motions. We have therefore essentially a three-dimensional system, hence a Bose-Einstein condensation.

$$= \frac{k^2 T}{\lambda^2 \sigma \Delta} [6g_3(1) - 6g_3(e^{-\beta \Delta}) - 2\beta \Delta g_2(e^{-\beta \Delta}) + \beta \Delta \ln(1 - e^{-\beta \Delta})],$$

$$T < T_c, \quad (46c)$$

where  $T_c$  is defined by

$$\lambda_c^2 \sigma \beta_c \Delta = g_2(1) - g_2(e^{-\beta_c \Delta}). \quad (47)$$

Equations (46a) and (46b) are precisely Eq. (4) of Ref. 27 provided that we identify

$$\begin{aligned} \Delta &\rightarrow V(R) \\ f_n &\rightarrow F_n^+ \end{aligned} \quad (48)$$

and

$$g_n \rightarrow F_n^-.$$

The expression Eq. (46c) for  $C_B, T < T_c$ , was not given in Ref. 27. Numerical results obtained<sup>(27)</sup> for  $\Delta/k=1^\circ$  and  $\sigma=0.026\text{\AA}^{-2}$  appear to be in qualitative agreement with experiment.

It is tempting to modify the above results by using distribution functions  $g(E)$  which do not cut off sharply. However, any function  $g(E)$  which vanishes at  $E=0$  would always lead to a discontinuous  $\frac{dz}{d\beta}$  for bosons, hence a heat capacity of the form shown in Fig. 5. Again, it is hopeful that the interactions between the adatoms may have the effect of smoothing out this discontinuity.

## 6. Elementary Excitation. Model

We are not content with the interpretation given in the preceding subsection, on account of aesthetic reasons if nothing else. If the specific heat anomaly is a consequence of inhomogeneities in the substrate, the experiment of Dash and co-workers would necessarily appear as a measurement of substrate properties. The intrinsic properties of the two-dimensional system would be completely masked by irrelevant, external, and irreproducible substrate oddities. This we are not willing to accept until all conceivable alternatives are ruled out.

One theoretically sophisticated model yet remains to be investigated. In the helium monolayer we see a system of strongly interacting particles and must invoke the tools of quantum many-body theory. We must understand the structure of the elementary excitations which propagate in a two-dimensional quantum liquid. It is clear that there will be more than one excitation branch even for  $\text{He}^4$ . The lack of Bose-Einstein condensation suggests the existence of a single particle excitation continuum, bounded below by  $\hbar^2 k^2 / 2m$ . There will also be a collective (phonon-roton) branch, which is linear at small  $k$  and terminates or

merges into the continuum at large  $k$ . Such a description in terms of multiple elementary excitations must be checked against formal theorems known from many-body theory, such as sum rules and linewidth analysis. Such theoretical studies are now under way and will be reported elsewhere in the near future.